1-1-2012

Purification, crystallization and X-ray diffraction analysis of human dynamin-related protein 1 GTPase-GED fusion protein

Eva Klinglmayr

Julia Wenger

Sandra Mayr

Ella Bossy-Wetzel
University of Central Florida

Sandra Puehringer

Acta Crystallographica Section F
Structural Biology and Crystallization Communications
ISSN 1744-3091

Purification, crystallization and X-ray diffraction analysis of human dynamin-related protein 1 GTPase-GED fusion protein

Eva Klinglmayr,[a]‡ Julia Wenger,[a]‡ Sandra Mayr,[a] Ella Bossy-Wetzel[b] and Sandra Puehringer[c,d]*

[a]Department of Molecular Biology, University of Salzburg, 5020 Salzburg, Austria, [b]Burnett School of Biomedical Sciences, College of Medicine, University of Central Florida, Orlando, FL 32816, USA, [c]Institute for Soft Matter and Functional Materials, Macromolecular Crystallography, Helmholtz-Zentrum Berlin für Materialien und Energie, 12489 Berlin, Germany, and [d]Department of Biology and Chemistry, Freie Universität Berlin, 14195 Berlin, Germany

‡ These authors contributed equally to this work.

Correspondence e-mail: sandra.puehringer@helmholtz-berlin.de

Received 12 July 2012
Accepted 16 August 2012

The mechano-enzyme dynamin-related protein 1 plays an important role in mitochondrial fission and is implicated in cell physiology. Dysregulation of Drp1 is associated with abnormal mitochondrial dynamics and neuronal damage. Drp1 shares structural and functional similarities with dynamin 1 with respect to domain organization, ability to self-assemble into spiral-like oligomers and GTP-cycle-dependent membrane scission. Structural studies of human dynamin-1 have greatly improved the understanding of this prototypical member of the dynamin superfamily. However, high-resolution structural information for full-length human Drp1 covering the GTPase domain, the middle domain and the GTPase effector domain (GED) is still lacking. In order to obtain mechanistic insights into the catalytic activity, a nucleotide-free GTPase-GED fusion protein of human Drp1 was expressed, purified and crystallized. Initial X-ray diffraction experiments yielded data to 2.67 Å resolution. The hexagonal-shaped crystals belonged to space group $P2_12_12$, with unit-cell parameters a = 53.59, b = 151.65, c = 43.53 Å, one molecule per asymmetric unit and a solvent content of 42%. Expression of selenomethionine-labelled protein is currently in progress. Here, the expression, purification, crystallization and X-ray diffraction analysis of the Drp1 GTPase-GED fusion protein are presented, which form a basis for more detailed structural and biophysical analysis.

1. Introduction

Mitochondria play a critical role in diverse biological processes such as ATP synthesis, calcium homeostasis and apoptosis (Wallace & Fan, 2010). These highly dynamic organelles undergo frequent fusion and fission to regulate their number, morphology, distribution and function (Bereiter-Hahn & Vöth, 1994; Youle, 2005; Chen & Chan, 2009). The dynamin-related proteins (DRPs) are responsible for maintaining this fusion–fission equilibrium. They represent a subfamily of the dynamin superfamily, a group of highly conserved large GTPases which are known for their ability to self-assemble into high-order ring-like or spiral-like oligomers and to display oligomerization-dependent GTPase activity (Praefcke & McMahon, 2004; Lackner *et al.*, 2009). Despite these common biochemical features, DRPs contain only three of the five domains typically found in the classical dynamins, *e.g.* dynamin-1: an N-terminal GTPase domain, a middle domain (MID) and a C-terminal GTPase effector domain (GED). Whereas the GTPase domain shows a high degree of sequence conservation throughout the superfamily, the MID and GED are more variable. Interestingly, the MID, together with intramolecular and intermolecular interactions formed by the GED, plays important roles during self-assembly (Hoppins *et al.*, 2007).

Dynamin-related protein 1 (Drp1), a key regulator of mitochondrial fission, has an additional unstructured region between the MID and GED. This so-called insert B or variable domain (VD) has been suggested to play an important role in Drp1 regulation and self-assembly (Heymann & Hinshaw, 2009; Strack & Cribbs, 2012; Fig. 1*a*). Drp1 is evolutionarily conserved throughout most kingdoms of life, indicating its fundamental importance to cell biology (Westermann,

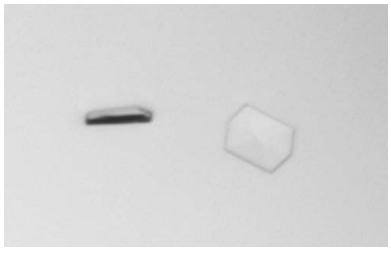

2010; Reddy *et al.*, 2011). *In vivo* studies with *drp1* knockout mice or mice carrying *drp1* mutations confirmed its essential role in cell survival (Wakabayashi *et al.*, 2009; Waterham *et al.*, 2007; Ishihara *et al.*, 2009). In humans, at least six different Drp1 isoforms are known, which are expressed in a tissue-specific and cell-type-specific manner (Reddy *et al.*, 2011; Ishihara *et al.*, 2009; Chang & Blackstone, 2010). *In vivo* and *in vitro* studies showed that Drp1 exists in a dimer–tetramer equilibrium in the cytoplasm (Shin *et al.*, 1999; Zhu *et al.*, 2004; Chang *et al.*, 2010; Bossy *et al.*, 2010). As a response to cellular stimuli, Drp1 is recruited to the mitochondrial outer membrane, where it self-assembles into spiral-like higher oligomeric structures at mitochondrial fission sites. These Drp1 clusters can be visualized as ribbons surrounding mitochondria or foci (Zhu *et al.*, 2004; Chang *et al.*, 2010; Frank *et al.*, 2001). Negative-stain electron microscopy revealed that Drp1 self-assembles into large spiral-shaped oligomers in the presence of GTP or nonhydrolysable GTP *in vitro* (Smirnova *et al.*, 2001; Song *et al.*, 2011; Yoon *et al.*, 2001). Studies using liposomes, which mimic the mitochondrial outer membrane, revealed Drp1 aggregation at membrane liposomes concurrent with membrane deformation (Yoon *et al.*, 2001). This finding suggests the involvement of Drp1 in membrane remodelling and scission. However, *in vitro* studies using Drp1 mutants and GTP analogues showed that GTP binding, but not GTP hydrolysis, is essential for oligomer assembly (Yoon *et al.*, 2001; Smirnova *et al.*, 2001). Indeed, it has been reported for the yeast homologue Dnm1 that the GTPase activity increases after assembly on liposomes followed by disassembly of the high-order oligomers (Ingerman *et al.*, 2005; Mears *et al.*, 2011; Mears & Hinshaw, 2008). Thus, GTP hydrolysis might induce a conformational change providing the mechanochemical work necessary for the mitochondrial fission process (Knott & Bossy-Wetzel, 2008; Otera & Mihara, 2011; Mears *et al.*, 2011).

Several factors that are required for membrane binding and regulation of Drp1 during this dynamic mechanism have already been identified (Dikov & Reichert, 2011; Otera *et al.*, 2010; Palmer *et al.*, 2011; Zhao *et al.*, 2011). Recent evidence also suggests that diverse post-translational modifications of Drp1 regulate mitochondrial fission (Chang & Blackstone, 2010; Oettinghaus *et al.*, 2012; Otera & Mihara, 2012; Elgass *et al.*, 2012; Chang *et al.*, 2010). However, their effects on Drp1 activity are incompletely understood and are a matter of current debate (Cho *et al.*, 2009; Bossy *et al.*, 2010; Chang & Blackstone, 2010).

Unravelling the molecular mechanism of human Drp1-mediated mitochondrial fission will allow us to modulate Drp1 activity in the pathogenesis of disease (Song *et al.*, 2011). For example, recent studies have revealed that excessive mitochondrial fission in degenerative diseases is caused by increased Drp1 activity (Knott *et al.*, 2008; Elgass *et al.*, 2012; Manczak & Reddy, 2012).

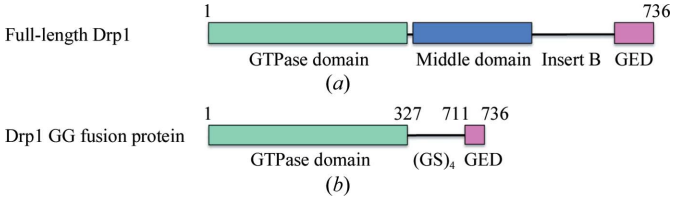

Figure 1
Construct design and schematic representation of the Drp1 GG fusion protein. (*a*) Full-length Drp1 consists of an N-terminal GTPase domain (green) and a helical middle domain (blue) followed by an unstructured region (insert B or variable domain) and a C-terminal GED (pink). (*b*) The GG fusion protein consists of the complete GTPase domain (amino acids 1–327) fused to a C-terminal fragment of the GED (amino acids 711–736) *via* a $(GS)_4$ linker.

High-resolution structural data for the human Drp1 GTPase domain will provide us with important insights into the mechanistic similarities and differences compared with dynamin-1. Construct design for the Drp1 GTPase domain was carried out on the basis of previously described GTPase-GED fusion protein structures of other dynamin superfamily members, such as human dynamin-1 (Chappie *et al.*, 2010) and a plant Drp1 homologue (Chen *et al.*, 2012). The Drp1 GG fusion protein shares 48 and 41% sequence identity with the GTPase-GED fusion proteins of human dynamin-1 (PDB entries 2x2e and 3zyc; Chappie *et al.*, 2010, 2011) and *Arabidopsis thaliana* Drp1A (*At*Drp1A; PDB entries 3t34 and 3t35; Yan *et al.*, 2011), respectively. Here, we report the expression, purification, crystallization and X-ray crystallographic characterization of a native fusion protein containing the GTPase domain and the C-terminal part of the GED of human Drp1.

2. Experimental methods

2.1. Cloning

To produce a stable and homogenous but still functional protein for crystallization experiments, the GTPase domain of human Drp1 (amino acids 1–327) was fused to the C-terminal part of the GED (amino acids 711–736) by a $(GS)_4$ linker (Fig. 1*b*). By removing the MID and the unstructured insert B the formation of higher-order oligomers was prevented and protein stability was increased. To generate the Drp1 GTPase-GED (GG) fusion construct the following four primers were designed: 5′-CTGGTCATATGGAGGCGCTA-ATTCCTGTC-3′ containing an *Nde*I restriction site, 5′-CTGGT-CTCGAGCCAAAGATGAGTCTCCCG-3′ containing an *Xho*I restriction site, 5′-GGTGAACCCGTGGATGGATCAGGATCAG-GATCAGGATCA-3′ and 5′-ATCAGCTGCTTCTTTTGATCCTG-ATCCTGATCCTGATCC-3′. The K38A mutation was introduced by overlap PCR using the mutagenic primers 5′-GAACGCAGAGC-AGCGGAGCAAGCTCAGTGCTAGAAAG-3′ and 5′-CTTTCTA-GCACTGAGCTTGCTCCGCTGCTCTGCGTTC-3′. Drp1 fragments were PCR-amplified from template DNA containing full-length Drp1 isoform 2 in pET21 (GenBank Accession No. NM_012063.2) using iProof High-Fidelity DNA Polymerase (Bio-Rad). The PCR product was digested with *Nde*I and *Xho*I and cloned into pET21 (Novagen), resulting in the attachment of two non-native amino acids (leucine and glutamic acid) and a His_6 tag at the C-terminus of the protein. The sequence was verified by DNA sequencing (Eurofins MWG Operon).

2.2. Expression

For protein expression, the Drp1 GG fusion construct and a construct containing a K38A substitution mutation in the GTPase domain rendering the Drp1 enzymatically inactive were transformed into *Escherichia coli* BL21 (DE3) Star cells and grown on LB plates containing 50 µg ml^{-1} ampicillin (Carl Roth) overnight at 310 K. Subsequently, cells were transferred into two Erlenmeyer flasks containing 600 ml LB medium with 50 µg ml^{-1} ampicillin and grown at 310 K with agitation at 230 rev min^{-1} until an OD_{600} of 0.8 was attained. After induction with 0.5 m*M* isopropyl *β*-thiogalactopyranoside (Carl Roth), expression was performed overnight at 298 K. The cells were harvested by centrifugation at 4500*g* for 20 min at 277 K. The cell pellets were dissolved in a 1/20 volume of lysis buffer [50 m*M* KH_2PO_4 pH 7.8, 300 m*M* NaCl, 10%(*v*/*v*) glycerol, 5 m*M* imidazole, 0.1 mg ml^{-1} lysozyme] and frozen at 253 K overnight before purification.

2.3. Protein purification

After thawing, the cells were lysed on ice by two cycles of sonication (Bandelin Electronic UW2070) at 70% of the maximum intensity amplitude for 3 min. DNA digestion was performed with 10 µg ml^{-1} DNase I (Fermentas) for 30 min at 293 K. The cell lysates were cleared by centrifugation at 18 000*g* for 20 min at 277 K. The supernatant was loaded onto Ni–NTA resin (GE Healthcare) pre-equilibrated in wash buffer [20 m*M* Tris pH 7.8, 300 m*M* NaCl, 40 m*M* imidazole, 10%(*v*/*v*) glycerol, 10%(*w*/*v*) sucrose]. To remove impurities, the nickel beads were washed with 30 column volumes of wash buffer. The protein was eluted with at least two column volumes of elution buffer [20 m*M* Tris pH 7.8, 300 m*M* NaCl, 10%(*v*/*v*) glycerol, 500 m*M* imidazole] and further purified on an ÄKTA FPLC system using a Superdex 75 10/300 GL column (GE Healthcare) pre-equilibrated with gel-filtration buffer (30 m*M* Tris pH 7.8, 100 m*M* NaCl, 2 m*M* DTT, 1 m*M* EDTA). The Drp1 GG fusion protein eluted as a monomer at a retention volume of approximately 11 ml (Fig. 2*a*) and displayed virtually no impurities (Fig. 2*b*). Amicon Ultra centrifugal filter units (10 kDa cutoff, Millipore) were used to concentrate the protein to 10 mg ml^{-1} and it was stored at 193 K. The protein concentration was determined by UV absorbance at 280 nm. Peptide mass fingerprinting (Toplab, Munich, Germany) unambiguously identified the native protein as the Drp1 GG fusion protein. Furthermore, the intact mass of 40.923 kDa determined by mass spectrometry (Toplab, Munich, Germany) corresponded well to the calculated mass of 40.956 kDa. Drp1 full-length isoform 2 was expressed and purified as described elsewhere (Song *et al.*, 2011).

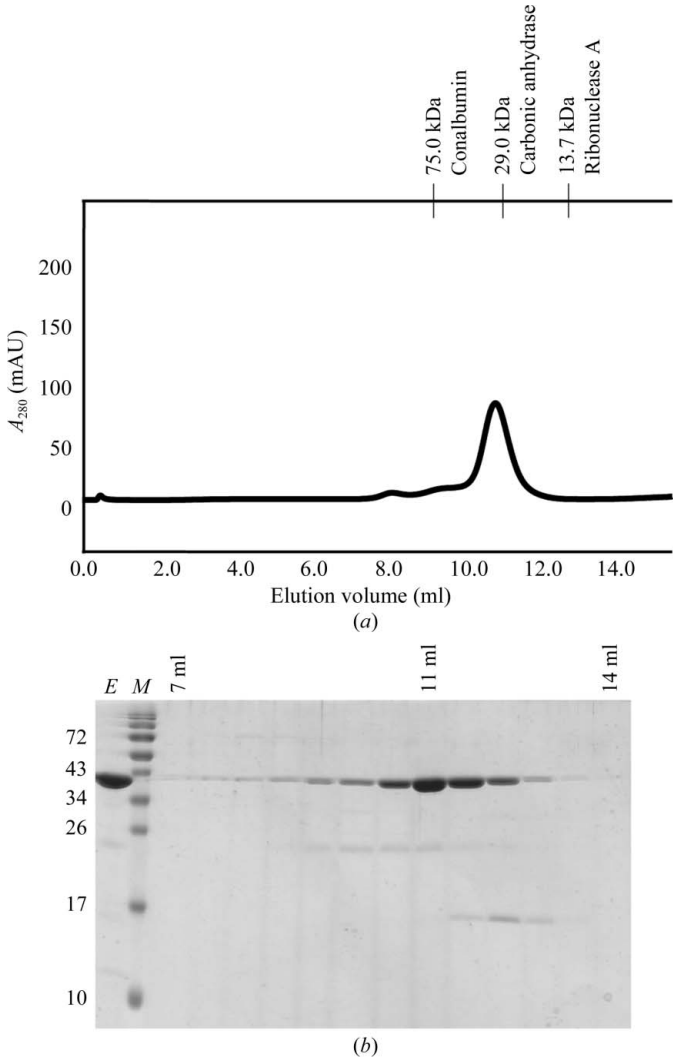

Figure 2
Purification of the Drp1 GG fusion protein. (*a*) Size-exclusion analysis. After Ni–NTA purification, proteins were loaded onto a Superdex 75 gel-filtration column and fractions containing protein were collected. In the absence of nucleotides, the protein eluted as a monomer at a retention volume of approximately 11 ml, which corresponds to a molecular mass of approximately 40 kDa. The retention volumes of molecular-mass standards (GE Healthcare) are displayed at the top. (*b*) SDS–PAGE analysis. Protein fractions were loaded onto a 15% SDS–PAGE gel and visualized by Coomassie Brilliant Blue staining. Lane *E*, eluted protein; lane *M*, protein molecular-mass markers (labelled in kDa on the left). The retention volumes are indicated at the top.

2.4. Drp1 GG fusion protein shows GTPase activity

The Drp1 GG fusion protein was tested for GTPase activity using the continuous regenerative coupled GTPase assay (Ingerman & Nunnari, 2005; Fig. 3). The protein was equilibrated in a buffer consisting of 25 m*M* HEPES/PIPES pH 7.0, 150 m*M* NaCl and was diluted to a concentration of 0.1 mg ml^{-1}. The absorbance (340 nm) correlating with NADH depletion at increasing GTP concentrations (0, 10, 20, 30, 50, 100, 250, 500 and 1000 µ*M*) was measured at 303 K for 85 min with 32 s per cycle using an Infinite M200 plate reader (Tecan). Drp1 full-length isoform 2 and the enzymatically inactive K38A GG fusion protein (Smirnova *et al.*, 1998) were used as positive and negative controls, respectively.

2.5. Protein crystallization

Crystallization of the Drp1 GG fusion protein (10 mg ml^{-1}) was performed in gel-filtration buffer using the sitting-drop vapour-diffusion method at 293 K. Commercial sparse-matrix screens such as Index (Hampton Research) and JCSG-*plus* (Molecular Dimensions) were used to screen for initial crystal hits. Drops were prepared by mixing 0.4 µl reservoir solution with 0.4 µl protein solution using a Hydra II Plus One (Matrix Ltd) liquid-handling system and were equilibrated against 50 µl reservoir solution in 96-well sitting-drop plates (Greiner). Stacks of thin crystal plates (Fig. 4*a*) were observed within 9 d in condition *A* [0.2 *M* lithium sulfate, 0.1 *M* bis-Tris pH 5.5, 25%(*v*/*v*) PEG 3350]. Furthermore, initial crystals in the form of clusters of needles were found in condition *B* (0.1 *M* sodium citrate pH 5.5, 20% PEG 3000).

Initial hits were refined manually by varying the buffer pH, the precipitant concentration or the protein concentration in 96-well plates. The crystals found in condition *A* were not reproducible,

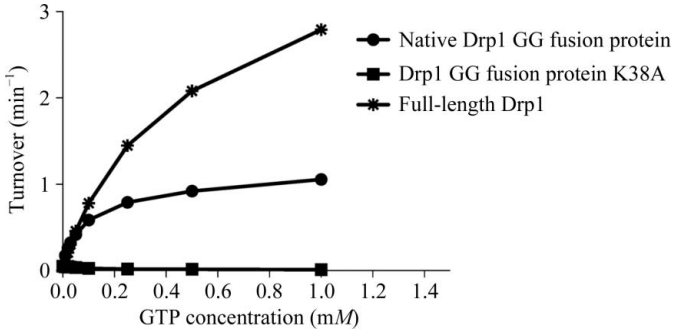

Figure 3
The Drp1 GG fusion protein displays GTPase activity: steady-state GTPase activities of Drp1 GG fusion protein (native Drp1 GG fusion protein) in comparison to Drp1 full-length isoform 2 and enzymatically inactive K38A mutant (Drp1 GG fusion protein K38A). Data are the mean ± standard deviation from three independent measurements.

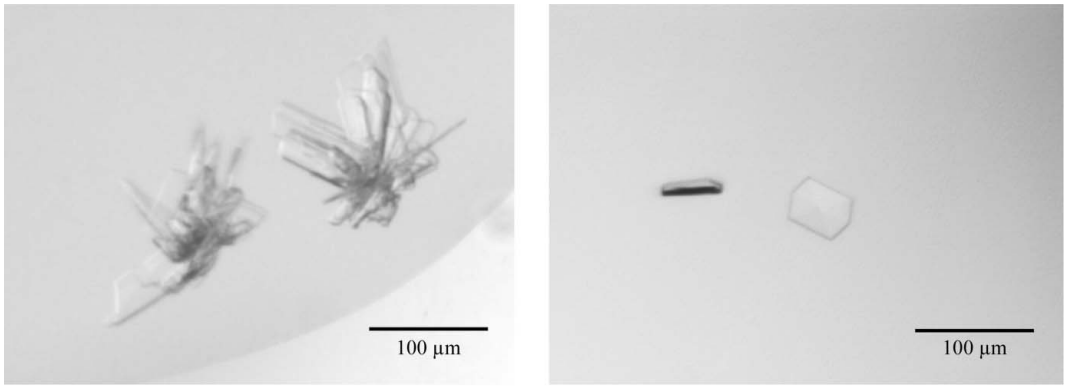

(*a*) (*b*)

Figure 4
Crystal forms of the Drp1 GG fusion protein. (*a*) In condition *A* only star-shaped intergrown crystals were present which could not be reproduced. (*b*) Reproducible crystals from condition *B* were only about 50 × 40 × 10 µm in size.

whereas a refined condition *B* (0.1 *M* sodium citrate pH 5, 27.5% PEG 3000) with a protein concentration of 1.2 mg ml^{-1}, a drop size of 0.8 µl and a 1:1 protein:reservoir solution ratio resulted in thin hexagonal-shaped crystals (Fig. 4*b*).

2.6. Data collection and processing

Refined crystals obtained using condition *B* were flash-cooled in liquid nitrogen without the addition of cryoprotectant. Diffraction data were collected on BL14.1 operated by the Helmholtz-Zentrum Berlin (HZB) at the BESSY II electron-storage ring (Berlin-Adlershof, Germany; Mueller *et al.*, 2012) at a wavelength of 0.91841 Å. A total of 180 diffraction images (Fig. 5) with an oscillation range of 1.0° were recorded using a Rayonics MX225 3 × 3 CCD detector at a distance of 236.4 mm.

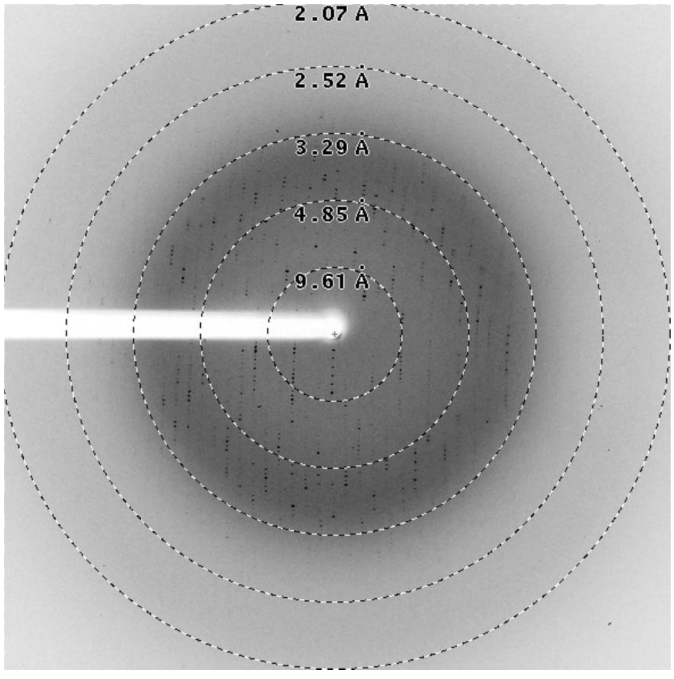

Figure 5
Diffraction image of the Drp1 GG fusion protein: a diffraction image of the crystals produced in condition *B* collected on BL14.1 at BESSY II, Berlin, Germany.

Table 1
Data-collection and processing statistics.

Values in parentheses are for the highest resolution shell.

Crystallization condition	0.1 *M* sodium citrate pH 5.5, 20% PEG 3000 [condition *B*]
Unit-cell parameters (Å, °)	a = 53.59, b = 151.65, c = 43.53, $\alpha = \beta = \gamma$ = 90.00
X-ray source	BL14.1, HZB, Berlin
Detector	Rayonics MX225 3 × 3 CCD
Space group	$P2_12_12$
Wavelength (Å)	0.91841
Crystal-to-detector distance (mm)	236.4
Exposure time per image (s)	15
$\Delta\varphi$ (°)	1.0
No. of images	180
Resolution (Å)	43.76–2.67 (2.83–2.67)
Reflections observed	76144 (11938)
Unique reflections	10686 (1678)
Multiplicity	7.13 (7.11)
Completeness of data (%)	99.8 (99.6)
$\langle I/\sigma(I)\rangle$	9.73 (2.16)
$R_{\rm merge}$† (%)	18.2 (93.6)
$R_{\rm r.i.m.}$‡ (%)	19.6 (100.9)
$R_{\rm p.i.m.}$§ (%)	7.3 (37.3)
Mosaicity (°)	0.35
Molecules per asymmetric unit	1
Solvent content (%)	42

† The merging R factor $R_{\rm merge} = \sum_{hkl}\sum_i |I_i(hkl) - \langle I(hkl)\rangle| / \sum_{hkl}\sum_i I_i(hkl)$, where $\langle I(hkl)\rangle$ is the mean of the i individual measurements $I_i(hkl)$ of the intensity of reflection hkl. ‡ The redundancy-independent merging R factor $R_{\rm r.i.m.} = \sum_{hkl}\{N(hkl)/[N(hkl)-1]\}^{1/2}\sum_i |I_i(hkl) - \langle I(hkl)\rangle| / \sum_{hkl}\sum_i I_i(hkl)$, where $\langle I(hkl)\rangle$ is the mean of the $N(hkl)$ individual measurements $I_i(hkl)$ of the intensity of reflection hkl. § The precision-indicating merging R factor $R_{\rm p.i.m.} = \sum_{hkl}\{1/[N(hkl)-1]\}^{1/2} \times \sum_i |I_i(hkl) - \langle I(hkl)\rangle| / \sum_{hkl}\sum_i I_i(hkl)$ (Weiss, 2001) calculated with the program *RMERGE* available upon request from M. S. Weiss.

All data were indexed, integrated, scaled and merged using *XDS* (Kabsch, 2010) using the *XDSAPP* graphical user interface (Krug *et al.*, 2012). For further information regarding data-collection and processing statistics, see Table 1.

3. Results and discussion

Structural information from other DRP-family members indicates that the C-terminus of the GED is necessary in order to interact with both the carboxy-terminus and the amino-terminus of the GTPase domain and to stabilize the GTPase domain (Chappie *et al.*, 2009). Therefore, a Drp1 GG fusion protein was designed by fusing the GTPase domain to the C-terminal part of the GED. The protein was cloned, expressed in *E. coli* and purified using a two-step

procedure. A continuous coupled GTPase activity assay showed that the human Drp1 GG fusion protein is an active enzyme. However, the GG fusion protein showed reduced GTPase activity in comparison to the full-length protein (Fig. 3). The observed difference in GTPase activities might be attributed to the inability of the Drp1 GG fusion protein to assemble into higher-order oligomers, preventing it from reaching maximal GTPase activity. According to the recently published GG fusion protein structures of human dynamin and *At*Drp1A (Chappie *et al.*, 2010; Yan *et al.*, 2011), we expect that the Drp1 GG fusion protein is able to dimerize *via* the GTPase domains but cannot form tetramers or GTPase-stimulating spiral-like structures.

Initial crystallization experiments were set up and after 9 d crystal plates could be observed in condition *A* consisting of 0.2 *M* lithium sulfate, 0.1 *M* bis-Tris pH 5.5, 25%(*v*/*v*) PEG 3350. Clusters of needles could be obtained in condition *B* consisting of 0.1 *M* sodium citrate pH 5.5, 20% PEG 3000 and gave three-dimensional hexagonal crystals after manual refinement of the conditions.

Crystals grown in condition *B* showed diffraction to 2.67 Å resolution and belonged to space group $P2_12_12$, with unit-cell parameters a = 53.59, b = 151.65, c = 43.53 Å. Calculation of the Matthews coefficient revealed one molecule in the asymmetric unit with a solvent content of 42% (Matthews, 1968). For additional information on data collection and processing, see Table 1. As molecular replacement using human dynamin GG fusion protein (PDB entry 2x2e) as the search model failed, expression of selenomethionine-labelled protein has been initiated.

Data collection was performed at the Helmholtz-Zentrum Berlin für Materialien und Energie Elektronenspeicherring BESSY II, Berlin, Germany and was supported by European Community's Seventh Framework Program (FP7/2007-2013) under grant agreement No. 226716. SP was supported by Erwin-Schrödinger Postdoc Fellowships from the Austrian Science Fund (J3173-N17). We thank the Austrian Science Fund (FWF W_01213) for financial support. EBW was supported by NIH grant R01 NS055195. Furthermore we would like to thank Christina Doppler for cloning the K38A mutant.

References

Bereiter-Hahn, J. & Vöth, M. (1994). *Microsc. Res. Tech.* **27**, 198–219.

Bossy, B., Petrilli, A., Klinglmayr, E., Chen, J., Lutz-Meindl, U., Knott, A. B., Masliah, E., Schwarzenbacher, R. & Bossy-Wetzel, E. (2010). *J. Alzheimers Dis.* **20**, S513–S526.

Chang, C.-R. & Blackstone, C. (2010). *Ann. N. Y. Acad. Sci.* **1201**, 34–39.

Chang, C.-R., Manlandro, C. M., Arnoult, D., Stadler, J., Posey, A. E., Hill, R. B. & Blackstone, C. (2010). *J. Biol. Chem.* **285**, 32494–32503.

Chappie, J. S., Acharya, S., Leonard, M., Schmid, S. L. & Dyda, F. (2010). *Nature (London)*, **465**, 435–440.

Chappie, J. S., Acharya, S., Liu, Y. W., Leonard, M., Pucadyil, T. J. & Schmid, S. L. (2009). *Mol. Biol. Cell*, **20**, 3561–3571.

Chappie, J. S., Mears, J. A., Fang, S., Leonard, M., Schmid, S. L., Milligan, R. A., Hinshaw, J. E. & Dyda, F. (2011). *Cell*, **147**, 209–222.

Chen, H. & Chan, D. C. (2009). *Hum. Mol. Genet.* **18**, R169–R176.

Chen, X., Xu, X., Sun, Y., Zhou, J., Ma, Y., Yan, L. & Lou, Z. (2012). *Acta Cryst.* F**68**, 69–72.

Cho, D. H., Nakamura, T., Fang, J., Cieplak, P., Godzik, A., Gu, Z. & Lipton, S. A. (2009). *Science*, **324**, 102–105.

Dikov, D. & Reichert, A. S. (2011). *EMBO J.* **30**, 2751–2753.

Elgass, K., Pakay, J., Ryan, M. T. & Palmer, C. S. (2012). *Biochim. Biophys. Acta*, doi:10.1016/j.bbamcr.2012.05.002.

Frank, S., Gaume, B., Bergmann-Leitner, E. S., Leitner, W. W., Robert, E. G., Catez, F., Smith, C. L. & Youle, R. J. (2001). *Dev. Cell*, **1**, 515–525.

Heymann, J. A. & Hinshaw, J. E. (2009). *J. Cell Sci.* **122**, 3427–3431.

Hoppins, S., Lackner, L. & Nunnari, J. (2007). *Annu. Rev. Biochem.* **76**, 751–780.

Ingerman, E. & Nunnari, J. (2005). *Methods Enzymol.* **404**, 611–619.

Ingerman, E., Perkins, E. M., Marino, M., Mears, J. A., McCaffery, J. M., Hinshaw, J. E. & Nunnari, J. (2005). *J. Cell Biol.* **170**, 1021–1027.

Ishihara, N. *et al.* (2009). *Nature Cell Biol.* **11**, 958–966.

Kabsch, W. (2010). *Acta Cryst.* D**66**, 125–132.

Knott, A. B. & Bossy-Wetzel, E. (2008). *Ann. N. Y. Acad. Sci.* **1147**, 283–292.

Knott, A. B., Perkins, G., Schwarzenbacher, R. & Bossy-Wetzel, E. (2008). *Nature Rev. Neurosci.* **9**, 505–518.

Krug, M., Weiss, M. S., Heinemann, U. & Mueller, U. (2012). *J. Appl. Cryst.* **45**, 568–572.

Lackner, L. L., Horner, J. S. & Nunnari, J. (2009). *Science*, **325**, 874–877.

Manczak, M. & Reddy, P. H. (2012). *Hum. Mol. Genet.* **21**, 2538–2547.

Matthews, B. W. (1968). *J. Mol. Biol.* **33**, 491–497.

Mears, J. A. & Hinshaw, J. E. (2008). *Methods Cell Biol.* **88**, 237–256.

Mears, J. A., Lackner, L. L., Fang, S., Ingerman, E., Nunnari, J. & Hinshaw, J. E. (2011). *Nature Struct. Mol. Biol.* **18**, 20–26.

Mueller, U., Darowski, N., Fuchs, M. R., Förster, R., Hellmig, M., Paithankar, K. S., Pühringer, S., Steffien, M., Zocher, G. & Weiss, M. S. (2012). *J. Synchrotron Rad.* **19**, 442–449.

Oettinghaus, B., Licci, M., Scorrano, L. & Frank, S. (2012). *Acta Neuropathol.* **123**, 189–203.

Otera, H. & Mihara, K. (2011). *Small GTPases*, **2**, 167–172.

Otera, H. & Mihara, K. (2012). *Int. J. Cell Biol.* **2012**, 821676.

Otera, H., Wang, C., Cleland, M. M., Setoguchi, K., Yokota, S., Youle, R. J. & Mihara, K. (2010). *J. Cell Biol.* **191**, 1141–1158.

Palmer, C. S., Osellame, L. D., Laine, D., Koutsopoulos, O. S., Frazier, A. E. & Ryan, M. T. (2011). *EMBO Rep.* **12**, 565–573.

Praefcke, G. J. & McMahon, H. T. (2004). *Nature Rev. Mol. Cell Biol.* **5**, 133–147.

Reddy, P. H., Reddy, T. P., Manczak, M., Calkins, M. J., Shirendeb, U. & Mao, P. (2011). *Brain Res. Rev.* **67**, 103–118.

Shin, H.-W., Takatsu, H., Mukai, H., Munekata, E., Murakami, K. & Nakayama, K. (1999). *J. Biol. Chem.* **274**, 2780–2785.

Smirnova, E., Griparic, L., Shurland, D. L. & van der Bliek, A. M. (2001). *Mol. Biol. Cell*, **12**, 2245–2256.

Smirnova, E., Shurland, D. L., Ryazantsev, S. N. & van der Bliek, A. M. (1998). *J. Cell Biol.* **143**, 351–358.

Song, W. *et al.* (2011). *Nature Med.* **17**, 377–382.

Strack, S. & Cribbs, J. T. (2012). *J. Biol. Chem.* **287**, 10990–11001.

Wakabayashi, J., Zhang, Z., Wakabayashi, N., Tamura, Y., Fukaya, M., Kensler, T. W., Iijima, M. & Sesaki, H. (2009). *J. Cell Biol.* **186**, 805–816.

Wallace, D. C. & Fan, W. (2010). *Mitochondrion*, **10**, 12–31.

Waterham, H. R., Koster, J., van Roermund, C. W., Mooyer, P. A., Wanders, R. J. & Leonard, J. V. (2007). *N. Engl. J. Med.* **356**, 1736–1741.

Weiss, M. S. (2001). *J. Appl. Cryst.* **34**, 130–135.

Westermann, B. (2010). *Nature Rev. Mol. Cell Biol.* **11**, 872–884.

Yan, L., Ma, Y., Sun, Y., Gao, J., Chen, X., Liu, J., Wang, C., Rao, Z. & Lou, Z. (2011). *J. Mol. Cell. Biol.* **3**, 378–381.

Yoon, Y., Pitts, K. R. & McNiven, M. A. (2001). *Mol. Biol. Cell*, **12**, 2894–2905.

Youle, R. J. (2005). *Dev. Cell*, **8**, 298–299.

Zhao, J., Liu, T., Jin, S., Wang, X., Qu, M., Uhlén, P., Tomilin, N., Shupliakov, O., Lendahl, U. & Nistér, M. (2011). *EMBO J.* **30**, 2762–2778.

Zhu, P.-P., Patterson, A., Stadler, J., Seeburg, D. P., Sheng, M. & Blackstone, C. (2004). *J. Biol. Chem.* **279**, 35967–35974.